Amino Acids (2012) 42:867–876
DOI 10.1007/s00726-011-1002-3

ORIGINAL ARTICLE

Constitutively and highly expressed *Oryza sativa* polyamine oxidases localize in peroxisomes and catalyze polyamine back conversion

Yusuke Ono · Dong Wook Kim · Kanako Watanabe · Ayano Sasaki · Masaru Niitsu · Thomas Berberich · Tomonobu Kusano · Yoshihiro Takahashi

Received: 28 February 2011 / Accepted: 7 April 2011 / Published online: 28 July 2011

Abstract Polyamine oxidases (PAOs) are FAD-dependent enzymes involved in polyamine (PA) catabolism. Recent studies have revealed that plant PAOs are not only active in the terminal catabolism of PAs as demonstrated for maize apoplastic PAO but also in a polyamine back-conversion pathway as shown for most Arabidopsis PAOs. We have characterized *Oryza sativa PAO*s at molecular and biochemical levels. The rice genome contains 7 *PAO* isoforms that are termed *OsPAO1* to *OsPAO7*. Of the seven PAOs, *OsPAO3*, *OsPAO4*, and *OsPAO5* transcripts were most abundant in 2-week-old seedlings and mature plants, while *OsPAO1*, *OsPAO2*, *OsPAO6*, and *OsPAO7* were expressed at very low levels with different tissue specificities. The more abundantly expressed PAOs—*OsPAO3*, *OsPAO4*, and *OsPAO5*—were cloned, and their gene products were produced in *Escherichia coli*. The enzymatic activities of the purified OsPAO3 to OsPAO5 proteins were examined. OsPAO3 favored spermidine (Spd) as substrate followed by thermospermine (T-Spm) and spermine (Spm) and showed a full PA back-conversion activity. OsPAO4 substrate specificity was similar to that of OsPAO5 preferring Spm and T-Spm but not Spd. Those enzymes also converted Spm and T-Spm to Spd, again indicative of PA back-conversion activities. Lastly, we show that OsPAO3, OsPAO4, and OsPAO5 are localized in peroxisomes. Together, these data revealed that constitutively and highly expressed *O. sativa* PAOs are localized in peroxisomes and catalyze PA back-conversion processes.

Keywords *Oryza sativa* · Peroxisome · Polyamine · Polyamine oxidase · Substrate specificity · Tissue specificity

Abbreviations

AO	Amine oxidase
Arg	Arginine
AtPAO	*Arabidopsis thaliana* polyamine oxidase
DAS	Day(s) after sowing
FAD	Flavin adenine dinucleotide
GFP	Green fluorescent protein
HvPAO	Barley polyamine oxidase
NorSpm	Norspermine
N^1-AcSpm	N^1-acetylspermine
Orn	Ornithine
PA	Polyamine
PAO	Polyamine oxidase
PCR	Polymerase chain reaction
OsPAO	*Oryza sativa* polyamine oxidase
PTS	Peroxisomal targeting signal
Put	Putrescine

Yusuke Ono and Dong Wook Kim were contributed equally to this work.

Electronic supplementary material The online version of this article (doi:10.1007/s00726-011-1002-3) contains supplementary material, which is available to authorized users.

Y. Ono · D. W. Kim · K. Watanabe · A. Sasaki · T. Kusano (✉) · Y. Takahashi (✉)
Graduate School of Life Sciences, Tohoku University, 2-1-1 Katahira, Aoba, Sendai, Miyagi 980-8577, Japan
e-mail: kusano@ige.tohoku.ac.jp

Y. Takahashi
e-mail: ytakahashi@ige.tohoku.ac.jp

M. Niitsu
Faculty of Pharmaceutical Sciences, Josai University, Sakado, Saitama 350-0295, Japan

T. Berberich
Biodiversity and Climate Research Center Frankfurt, Frankfurt, Germany

Spd	Spermidine
Spm	Spermine
T-Spm	Thermospermine
ZmPAO	Maize polyamine oxidase

Introduction

Polyamines (PAs) are small aliphatic amines constituting triamine spermidine (Spd), tetraamine spermine (Spm), and their diamine precursor putrescine (Put), the most common PAs widely found in both prokaryotes and eukaryotes including plants (Alcázar et al. 2010; Cohen 1998; Kusano et al. 2008; Mattoo et al. 2010; Tabor and Tabor 1985). Recent studies revealed the presence of another tetraamine, thermospermine (T-Spm) (Kakehi et al. 2008; Knott et al. 2007; Naka et al. 2010). Those plant PAs have been suggested to play important roles in various physiological processes such as embryogenesis, cell division, organogenesis, flowering and senescence, and also in responses to environmental stresses (Alcázar et al. 2010; Groppa and Benavides 2008; Kusano et al. 2008; Mattoo et al. 2010). The plant PA biosynthetic pathway has been well elucidated, and all the enzymes involved in PA biosynthesis and the corresponding genes were identified in Arabidopsis (Bagni and Tassoni 2001; Fuell et al. 2010; Kusano et al. 2008). PA biosynthesis starts from ornithine (Orn) or arginine (Arg). Orn is decarboxylated by Orn decarboxylase to produce Put. Arg is converted to Put via agmatine by three sequential reactions catalyzed by Arg decarboxylase, agmatine iminohydrolase, and N-carbamoylputrescine amidohydrolase. Put is converted to Spd by Spd synthase through the transfer of an aminopropyl group from decarboxylated S-adenosylmethionine, which is synthesized from methionine in two sequential reactions of methionine adenosyltransferase and S-adenosylmethionine decarboxylase, respectively. Triamine Spd is further converted to two tetraamine isomers Spm and T-Spm, and each reaction is catalyzed by Spm synthase and T-Spm synthase (ACAULIS5 or ACL5), respectively (Alcázar et al. 2010; Hanzawa et al. 2000; Hanzawa et al. 2002).

Comparatively, knowledge on PA catabolic pathway(s) in plants is fragmentary (Bassard et al. 2010; Cona et al. 2006; Tassoni et al. 2000) in regard to mammalian systems (Seiler 2004; Vujcic et al. 2002, 2003; Wallace et al. 2003; Wang et al. 2001). Diamine oxidase and polyamine oxidase (PAO, EC 1.5.3.11) are two enzymes involved in the PA catabolic process (Bagni and Tassoni 2001; Bassard et al. 2010; Cona et al. 2006). PAO is a flavin adenine dinucleotide (FAD)-dependent enzyme. It catalyzes the oxidative deamination of PAs at the secondary amino group (Cona et al. 2006; Federico and Angelini 1991; Wu et al. 2003). The initially characterized monocotyledonous plant PAOs such as maize PAO (ZmPAO) and barley PAO (HvPAOs) produced the corresponding aldehyde along with 1,3-diaminopropane and H_2O_2 (Cervelli et al. 2000, 2004, 2006; Cona et al. 2006; Federico and Angelini 1991), indicating that they are involved in the terminal catabolism of PAs (Binda et al. 1999; Cona et al. 2005; Tavladoraki et al. 1998). At least four Arabidopsis PAOs, namely AtPAO1 to AtPAO4, catalyze the conversion of Spm and T-Spm to Spd and/or Spd to Put, respectively, which provided evidence for the existence of a PA back-conversion pathway in plants (Fincato et al. 2011; Kamada-Nobusada et al. 2008; Moschou et al. 2008; Takahashi et al. 2010; Tavladoraki et al. 2006). Thus, plant PAOs can either be active in the terminal catabolism of PAs or in PA back conversion.

The question arises whether a single plant harbors both the PA catabolic pathways. From this point of view, we have focused in this study on a monocotyledonous model plant, *Oryza sativa*, examining its seven *PAO* isoforms and their gene products at molecular and biochemical levels. First, the tissue specificity of *OsPAO*s expression at two different growth stages of rice plants is addressed. Second, the cDNAs of the more abundantly expressed three *OsPAO* members were cloned and expressed in *Escherichia coli*. The PA specificity of the resulting OsPAOs and the reaction products are identified. Lastly, data on the cellular localization of the three OsPAOs are presented.

Materials and methods

Plant materials and growth condition

Rice plants (*Oryza sativa* cv. Nipponbare, provided by Hokuriku Agricultural Experimental Station) were grown hydroponically in two-fifths strength Hoagland's solution #2 [2 mM $Ca(NO_3)_2{\cdot}4H_2O$, 2 mM KNO_3, 0.8 mM $MgSO_4{\cdot}7H_2O$, 0.0002% $FeSO_4{\cdot}$EDTA] in a plant incubator (NK system, Nippon Medical and Chemical Instruments Co. Ltd, Tokyo, Japan). To get mature plant samples, seeds were pre-germinated in an incubator set at 30°C for 2 days, and then, each seed sown at the center of a plastic basket filled with tap water. Seven days after sowing (DAS), the tap water was replaced with a half strength Kimura B hydroponic solution [0.18 mM $(NH_4)_2SO_4$, 0.27 mM $MgSO_4$, 0.09 mM KNO_3, 0.18 mM $Ca(NO_3)_2$, 0.09 mM KH_2PO_4, 0.02 mM Fe–Na-EDTA, pH 5.0 adjusted with H_2SO_4]. The solution was replaced with normal-strength Kimura B solution at 21 DAS and exchanged every 2 days. The rice plants were grown in a greenhouse under natural lighting conditions (average air temperature, 30°C).

Real-time RT-PCR analysis

Total RNA was extracted from the respective tissues from 2-week-old rice seedlings or mature plants using Sepasol-RNA I Super (Nacalai Tesque, Kyoto, Japan). First-strand cDNA was synthesized with ReverTra Ace (Toyobo Co. Ltd., Osaka, Japan) and oligo-dT primers. Quantitative real-time RT-PCR was performed with Fast-Start Universal SYBR Green Master (ROX) (Roche Applied Science, Mannheim, Germany) on a StepOne real-time polymerase chain reaction (PCR) system (Life Technologies Japan, Tokyo, Japan). The *OsPAO*s' primers were designed by Primer Express® Software Version 3.0 (Applied Biosystems) and are listed in Table S1. They were used for the two-step real-time RT-PCR that was performed with the following program: one cycle of 94°C for 10 min, followed by 40 cycles of 94°C for 15 s and 60°C for 60 s. *O. sativa EF-1α* was used as an internal control for the assays. The amount of cDNA was calculated relative to the signals of a standard dilution of the respective PCR products using StepOne™ v2.1 (Applied Biosystems).

Preparation of recombinant OsPAO3, OsPAO4, and OsPAO5 proteins in *E. coli*

The coding regions of *OsPAO3, OsPAO4,* and *OsPAO5* were amplified by RT-PCR from total RNA of *O. sativa* young seedlings using gene-specific primers: *OsPAO3*, 5′-ACCGAGCTCATGGCGAACAACAGTTCA-3′ (forward, *Sac*I site underlined) and 5′-CTGAAGCTTTCACAGCCG GGAGATGAG-3′ (reverse, *Hin*dIII site underlined); *OsPAO4*, 5′-GCGCATATGGATCCCAATAGCCTCA-3′ (forward, *Nde*I site underlined) and 5′-TCAGTCGACT CAGGTCCTGCAAATCTG-3′ (reverse, *Sal*I site underlined); *OsPAO5*, 5′-GGGGGTACCATGGACCAGCCTT CTAAT-3′ (forward, *Kpn*I site underlined) and 5′-GTT TCTAGATCACAGCCTGGATATCTG-3′ (reverse, *Xba*I site underlined). Amplified PCR products were digested with the respective restriction enzymes and cloned in frame with the 6×His tag of the pCold vector (Takara Bio Inc., Shiga, Japan), resulting in pCold-*OsPAOs*. After confirming the cloned fragments by DNA sequencing, pCold-*OsPAOs* were transformed into *E. coli* BL21 (DE3) cells and the recombinant OsPAO proteins containing the N-terminal 6xHis tag expressed according to the pCold vector manufacturer's instructions (Takara Bio Inc., Shiga, Japan). The *E. coli* cells were collected by centrifugation and resuspended in 1/10 culture volumes of 50 mM phosphate buffer (pH 7.0), 300 mM NaCl, 1 mM phenylmethylsulfonyl fluorideimidazole, 1 mM β-mercaptoethanol, and disrupted by sonication. After centrifugation at 15,000 × *g* for 10 min at 4°C, the cleared supernatant was applied to a Ni–Agarose column to bind the recombinant protein. The column was washed with washing buffer [25 mM phosphate buffer (pH 7.0), 300 mM NaCl, 20 mM, 1 mM β-mercaptoethanol], and the bound proteins were eluted with elution buffer [25 mM phosphate buffer (pH 7.0), 300 mM NaCl, 300 mM imidazole, 1 mM β-mercaptoethanol]. The purified recombinant OsPAO proteins were immediately dialyzed overnight against 50 mM Tris–HCl (pH 8.0), 300 mM NaCl.

PAO activity assay

The catalytic activities of recombinant OsPAO3, OsPAO4, and OsPAO5 proteins for the oxidation of Spm, T-Spm, Spd, Put, N^1-AcSpm, and NorSpm were determined as described previously (Takahashi et al. 2010; Tavladoraki et al. 2006). In a typical experiment, 0.5–3 µg protein was added to a buffered solution (100 mM phosphate buffer, pH 7.0) containing the substrate (500 µM), 4-aminoantipyrine (100 µM), 3,5-dichloro-2-hydroxybenzesulfonic acid (1 mM), and horseradish peroxidase (10 U/ml), and the increase in absorbance at 515 nm was monitored.

Analysis of reaction products catalyzed by OsPAO3, OsPAO4, and OsPAO5

To determine the reaction products of PA oxidation, purified recombinant OsPAO3, OsPAO4, or OsPAO5 were incubated with 150 µM PA (Spm, T-Spm, or Spd) in 100 mM Tris–HCl (pH 8.0) at 30°C for various time points. The reaction was stopped by adding 9 times volume of 5% perchloric acid. The reaction products were benzoylated and analyzed by HPLC as previously described (Naka et al. 2010). Briefly, 1 ml of 2 N NaOH was added to 1 ml of reaction product, mixed, then 10 µl of benzoyl chloride was added, mixed, and incubated at room temperature for 20 min. After addition of 2 ml saturated sodium chloride and 2 ml of diethyl ether followed by strong mixing, phases were separated by centrifugation at 1,500 × *g* for 5 min at 4°C. Aliquots of the organic solvent phase (1.5 ml each) were evaporated, and the residue was resuspended in 50 µl of methanol. The benzoylated PAs were analyzed with a programmable Hewlett Packard series 1100 liquid chromatograph using reverse-phase column (4.6 × 250 mm, TSK-GEL ODS-80Ts, TOSOH, Tokyo, Japan) and detected at 254 nm. One cycle of the run resume is consisting of 60 min at a flow rate of 1 ml/min at 30°C, i.e., 42% acetonitrile for 25 min for PA separation, increased up to 100% acetonitrile during 3 min, 100% acetonitrile for 20 min for washing, decreased down to 42% acetonitrile during 3 min, then 42% acetonitrile for 9 min.

Construction of GFP fusion plasmids, particle bombardment, and microscopic observation in onion cells

First, the basal GFP vector was constructed. The coding region of GFP was amplified by PCR with pGFP2 (provided by Dr. N.-H. Chua) as a template and the following primer pair (forward, 5′-CTTGGATCCAAGGAGATATAAGAA TGGGTAAGGGAGAAGAACTTTTC-3′; reverse, 5′-TAT CCCGGGGCCCCCAGAGCCTCCTTTGTATAGTTCAT CCATGCCATG-3′) in which the underlined sequences was added for cloning purpose. The *Bam*HI- and *Sma*I-digested fragment were subcloned into the corresponding sites of the pBI221 vector (Invitrogen), yielding pBI221GFP. Next, the internal single *Sac*I site of *OsPAO4*- or *OsPAO5*-coding region was mutated without changing the amino acid sequence by two-step PCR using the following primer pairs: first, PCR with two primer pairs, in case of *OsPAO4*, OsPAO4-GFP-SacM-F (5′-GGAAGAGTTCTGCAATCG CAGACC-3′, the mutated site is underlined) and OsPAO4-GFP-Rv (5′-TTGGAGCTCTCAGGTCCTGCAAATCTG AAGG-3′, *Sac*I site is underlined), and OsPAO4-GFP-Fw (5′-GAACCCGGGATGGATCCCAATAGCCTCAAAA-3′, *Sma*I site is underlined) and OsPAO4-GFP-SacM-Rv (5′-TGCAGAACTCTTCCATGAGGGCAA-3′, the mutated site is underlined). Similarly, in case of *OsPAO5*, first PCR with OsPAO5-GFP-SacM-Fw (5′-ACCTGAACTC CCAGATTGGAAGCT-3′, the mutated site is underlined) and OsPAO5-GFP-Rv (5′-AATGAGCTCTCACAGCCT GGATATCTGGAAGGGG-3′, *Sac*I site is underlined), and OsPAO5-GFP-Fw (5′-TATCCCGGGATGGACCAG CCTTCTAATGGCT-3′, *Sma*I site is underlined) and OsPAO5-GFP-SacM-Rv (5′-CTGGGAGTTCAGGTTCA AACTTGA-3′, the mutated site is underlined). Then, second PCR on the respective mixtures of the first PCR products with the usage of the primers, OsPAO4-GFP-Fw and OsPAO4-GFP-Rv, and OsPAO5-GFP-Fw and OsPAO5-GFP-Rv, respectively, was performed. The coding region of *OsPAO3* was amplified by PCR using the following primer pair: OsPAO3-GFP-Fw (5′-GCCCCCG GGATGGCGAACAACAGTTCATATG-3′, *Sma*I site is underlined) and OsPAO3-GFP-Rv (5′-GGTGAGCTC TCACAGCCGGGAGATGAGCAGT-3′, *Sac*I site is underlined). The resulting *OsPAO3*, *OsPAO4,* and *OsPAO5* fragments digested with *Sma*I and *Sac*I were subcloned into the same restriction enzyme sites of pBI221GFP, yielding pBI221GFP-OsPAO3, pBI221GFP-OsPAO4, and pBI221GFP-OsPAO5, respectively. The resulting GFP-OsPAOs constructs were delivered into onion bulbs by particle bombardment. After incubating the bulbs at 22°C for 16 h in darkness, the epidermal layers were peeled off and observed with a fluorescence microscope (BX61; Olympus).

Results

Seven *PAO* isoforms are present in *Oryza sativa*

Seven *PAO* isoforms were revealed from the *Oryza sativa* genome analyzing the public database. Here, we numbered the PAO genes consecutively, in terms of the number of the chromosome on which the gene is located. Genes located on the same chromosome were numbered in descending order by their assigned accession number (Table 1). The gene products from the corresponding *OsPAOs*' cDNAs were termed OsPAO1 to OsPAO7. Phylogenetic analysis of the amino acid sequences of the seven *O. sativa* PAOs, five Arabidopsis PAOs, and several other plant PAOs was performed (Fig. 1). Plant PAOs were divided into four clades; clade I includes Arabidopsis AtPAO1, tobacco NtPAO (Yoda et al. 2006), and apple MdPAO1. Clade II comprises the three rice members, OsPAO2, OsPAO6, and OsPAO7, along with maize ZmPAO (Tavladoraki et al. 1998), barley HvPAO1, and HvPAO2 (Cervelli et al. 2001). Clade III is built by OsPAO1, *Brassica juncea* BjPAO (Lim et al. 2006), and AtPAO5. In clade IV, three rice PAOs, OsPAO3, OsPAO4, and OsPAO5 were grouped together with Arabidopsis peroxisome-localized members, AtPAO2, AtPAO3, and AtPAO4 (Kamada-Nobusada et al. 2008; Moschou et al. 2008). Clade I is dicotyledon-specific, and clade II members are all derived from monocotyledonous plants. In clades III and IV, both mono- and dicotyledonous PAOs grouped together.

Table 1 Nomenclature of seven *PAO* isoforms found in *O. sativa*

New name	Gene locus	Accession number	Former name
OsPAO1	Os01g0710200	NM_001050573	*OsAO4*
OsPAO2	Os03g0193400	NM_001055782	–
OsPAO3	Os04g0623300	NM_001060458	*OsAO3*
OsPAO4	Os04g0671200	NM_001060753	*OsAO1*
OsPAO5	Os04g0671300	NM_001060754	*OsAO2*
OsPAO6	Os09g0368200	NM_001069545	*OsPAO2*
OsPAO7	Os09g0368500	NM_001069546	*OsPAO3*

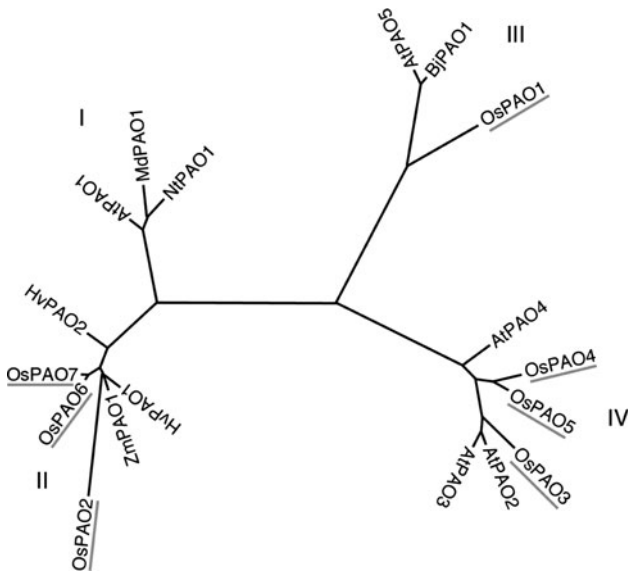

Fig. 1 Phylogenetic relationships of seven OsPAOs and other plant PAOs. Based on amino acid sequence alignment, the unrooted tree was drawn with the aid of molecular evolutionary genetics analysis (MEGA) software version 5.0 (Kumar et al. 2008). Seven *Oryza sativa* PAOs were highlighted with *gray solid lines*. *Roman letter* indicates the clade. The genes and accession numbers used were as follows: *OsPAO1* (NM_001050573); *OsPAO2* (NM_001055782); *OsPAO3* (NM_001060458); *OsPAO4* (NM_001060753); *OsPAO5* (NM_001060754); *OsPAO6* (NM_001069545); *OsPAO7* (NM_001069546); *AtPAO1* (At5g13700, NM_121373); *AtPAO2* (At2g43020, AF364952); *AtPAO3* (At3g59050, AY143905); *AtPAO4* (At1g65840, AF364953); *AtPAO5* (At4g29720, AK118203); *ZmPAO1* (*Zea mays PAO1*, NM_001111636); *NtPAO* (*Nicotiana tabacum PAO*, AB200262); *HvPAO1* (*Hordeum vulgare PAO1*, AJ298131); *HvPAO2* (*Hordeum vulgare PAO2*, AJ298132); *MdPAO* (*Malus domestica PAO*, AB250234); *BjPAO* (*Brassica juncea PAO,* AY188087)

Tissue specificity of seven *OsPAOs* in *O. sativa*

Using two different growth stages of rice plants, expression analysis of seven *OsPAO* members was performed. In two-week-old seedlings, *OsPAO3* was ubiquitous and highly expressed. Most abundant expression of *OsPAO3* was observed in youngest, fresh leaves (Fig. 2a). *OsPAO4* and *OsPAO5* transcripts were also abundantly expressed, but the expression specificity was different. These three *PAO*s categorized into clade IV (Fig. 1). Constitutively, low levels of *OsPAO1* expression were observed. *OsPAO2* and *OsPAO7* expression was observed in root at low levels. *OsPAO6* expression was detected at null levels (Fig. 2a). The latter three *PAO* members were grouped to clade II (Fig. 1). In mature flowering rice plants, the predominantly expressed members were *OsPAO3*, *OsPAO4*, and *OsPAO5* (Fig. 2b). Concerning their expression in different tissues, higher levels of *OsPAO3* transcripts were detected in rachis, node, and lower leaf blade, *OsPAO4* in rachis, and *OsPAO5* in flag leaf, lower leaf blade, and basal part of leaf sheath (Fig. 2b). Highest expression of *OsPAO1* was observed in rachis. The remaining members—*OsPAO2*, *OsPAO6*, and *OsPAO7*—were expressed at negligible levels (Fig. 2b).

Production of OsPAO3, OsPAO4, and OsPAO5 in *E. coli* and substrate specificity of their enzymes

The cDNAs of *OsPAO3*, *OsPAO4*, and *OsPAO5*, which were expressed at higher levels among the members, were cloned into pCold vector (Takara) and the genes expressed in *E. coli* as His-tagged proteins. OsPAO3 was purified to homogeneity (Fig. 3a). Measurement of spectrum absorption in a range of 300–540 nm of this preparation showed two absorption maxima at almost 380 and 460 nm, indicative of typical feature of a FAD-contained protein (Fig. 3b). The enzymatic activity of the recombinant OsPAO3 was determined with various PAs. OsPAO3 oxidized Spm, T-Spm, and Nor-Spm, but its most preferred substrate was Spd (Fig. 3c). Put was a poor substrate for OsPAO3. In Fig. 3d, time-dependent change in the concentration of the substrate Spm is shown. This enzyme likely converts Spm to Spd, then to Put, indicating that OsPAO3 has a full PA back-conversion activity.

OsPAO4 was also purified to homogeneity (Fig. 4a) and showed absorption spectra-specific to a FAD protein (Fig. 4b). OsPAO4 recombinant protein utilized Spm and T-Spm as favorable substrates (Fig. 4c). When Spm was used as a substrate for the purified OsPAO4, Spd was produced in a time-dependent manner (Fig. 4d, data not shown). Thus, OsPAO4 also seems to function in PA back-conversion process.

In the case of OsPAO5, the recombinant protein was less soluble even in the cold-inducible expression system. Thus, the purity of the preparation was not complete as judged by SDS–PAGE and spectrum absorption (Figs. 5a, b). However, we assayed the PA specificity using this preparation. OsPAO5 shares high identity (76%) with OsPAO4, and their PA specificity was quite similar, i.e., OsPAO5 preferred Spm > T-Spm > Nor-Spm while it did not use Spd, Put, and N^1-AcSpm as substrates (Fig. 5c). OsPAO5 converted Spm to Spd in a time-dependent manner, but did not produce Put (Fig. 5d, data not shown). Thus, we suggest that the three OsPAOs of clade IV all have the capacity to back convert PAs.

Cellular localization of OsPAO3, OsPAO4, and OsPAO5

Arabidopsis AtPAO2, AtPAO3, and AtPAO4 being categorized in clade IV in this study were localized in peroxisomes (Kamada-Nobusada et al. 2008; Moschou et al. 2008). OsPAO3, OsPAO4, and OsPAO5 also belong to this

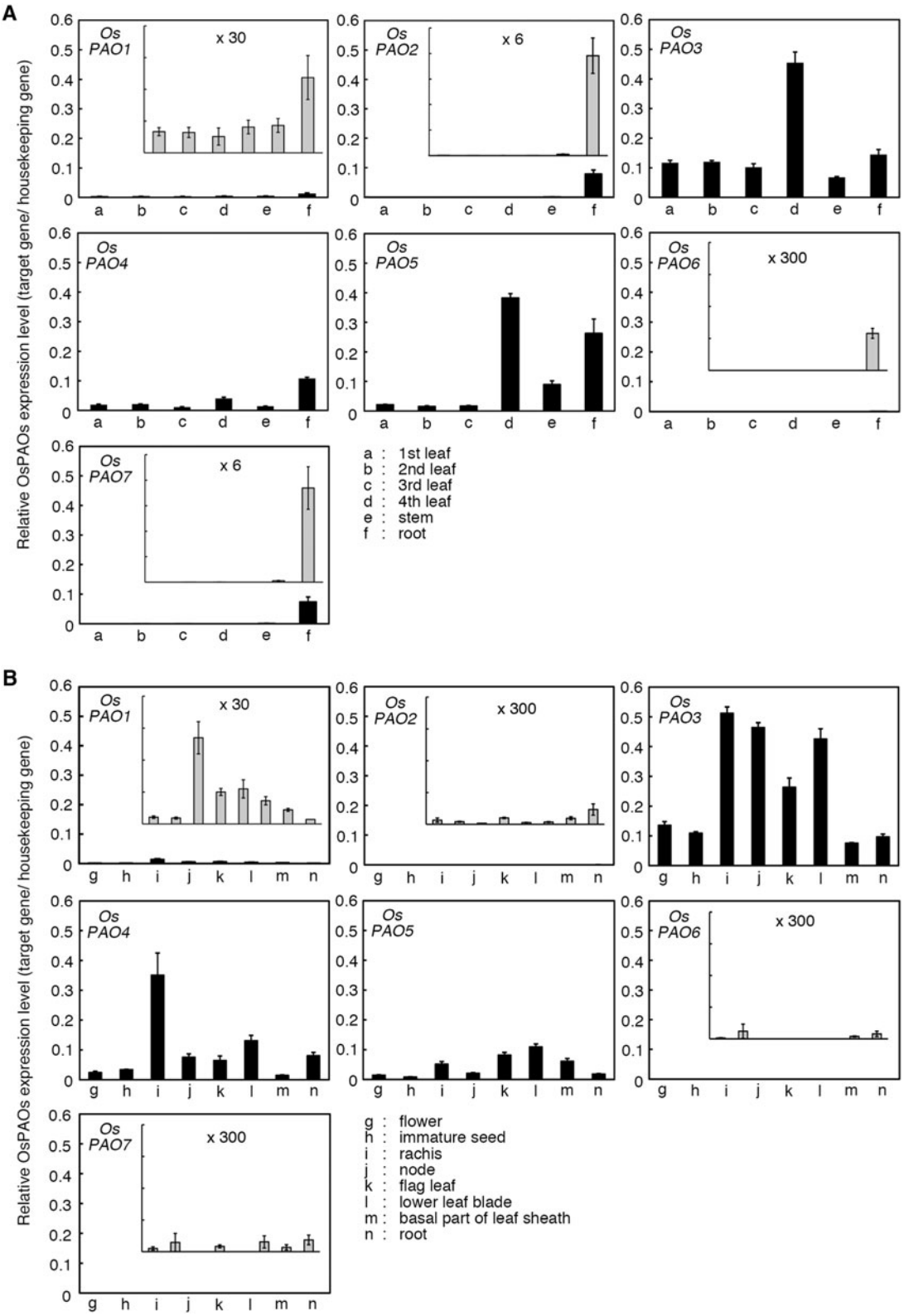

Fig. 2 Tissue-specific expression of seven *O. sativa PAO* genes at two different growth stages. The transcript levels in the corresponding tissues were quantified by real-time RT-PCR using gene-specific primers designed for *OsPAO1* to *OsPAO7* (see supplemental Table S1) and normalized to a control gene, *EF-1α*. **a** 2-week-old seedlings. *a*, first leaf; *b*, second leaf; *c*, third leaf; *d*, fourth youngest leaf; *e*, leaf sheath; *f*, root. **b** Rice plants at flowering stage. *g*, flower; *h*, immature seed; *i*, rachis; *j*, node; *k*, flag leaf; *l*, lower leaf blade; *m*, basal part of leaf sheath; *n*, root. The insets have magnified scales in ordinates, i.e., maximum scales are 0.1 (in case of × 6), 0.02 (×30), and 0.002 (×300), respectively

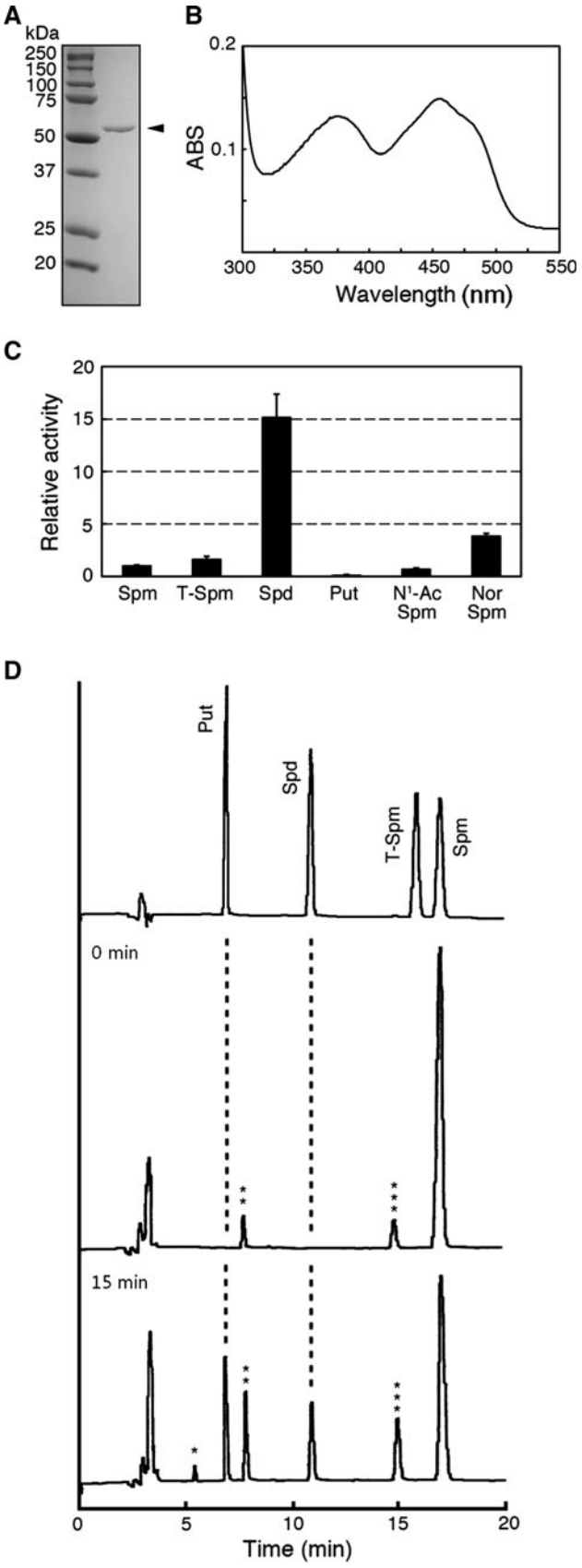

◄ **Fig. 3** Biochemical characteristics of OsPAO3. **a** Purification of the recombinant OsPAO3 protein on SDS–PAGE and visualized by CBB-staining. **b** Absorption spectrum of the purified OsPAO3 in a range of 300–540 nm. **c** PA specificity of the recombinant OsPAO3. The OsPAO3 enzyme activity was assessed by H_2O_2 production using the individual PAs as substrates. Activities were displayed relative to the one detected with Spm that was set as 1. **d**. HPLC analysis of the reaction products catalyzed by OsPAO3 when Spm was used as a substrate

clade (Fig. 1). When these six members were sequence-aligned, their carboxy-distal sequences displayed putative type I peroxisomal targeting signals (PTS1). PTS1 is a C-terminal tripeptide consisting of the consensus sequence (S/A/C)(K/R/H)(L/M). In plants, the preferred targeting signal is SKL (highlighted by red asterisks in Fig. 6a; Reumann et al. 2007; Zolman and Bartel 2004). OsPAO3 and OsPAO5 contain the SRL sequences that are identical with that of AtPAO2. OsPAO4 has the CRT sequence. Thr is a synonymous substitution of Leu/Met, so we predicted that OsPAO4 also targets to peroxisomes. To follow this up, green fluorescent protein (GFP)-fusion approach was taken. GFP-OsPAOs fusion constructs were biolistically bombarded into onion bulbs. We employed mCherry-AtPAO3, provided by Dr. Roubelakis-Angelakis (University of Crete), as a positive marker for peroxisomes. Green fluorescence derived from GFP-OsPAO3 localized in small dotted-like organelles in which red fluorescence derived from the peroxisome-positive marker construct was localized (Fig. 6b, second column). Green fluorescence derived from GFP-OsPAO4 and GFP-OsPAO5 also co-localized with red fluorescence derived from mCherry-AtPAO3 (Fig. 6b, third and fourth columns). These results provide evidence in support of *O. sativa* PAO members belonging to clade IV as localized in peroxisomes.

Discussion

In the present study, we documented the expression profiles in various tissues of seven *O. sativa PAO* genes. We also characterized the enzymatic features and cellular localization of OsPAO3, OsPAO4, and OsPAO5 expressed in a heterologous system. Transcriptional analysis uncovered that the PAO members that classified into clade II of the phylogenetic tree, *OsPAO2*, *OsPAO6,* and *OsPAO7*, were expressed at low levels under given physiological conditions (Fig. 2). The other members of this clade, maize *ZmPAO* and barley *HvPAO1*, were shown to be induced by wounding (Angelini et al. 2008) and had an ear-specific expression (Cervelli et al. 2006), respectively. Thus, *OsPAO2*, *OsPAO6*, and *OsPAO7* may be expressed either in restricted tissues/organs or stress-inducible manner. ZmPAO and HvPAO1 are apoplastic enzymes, while

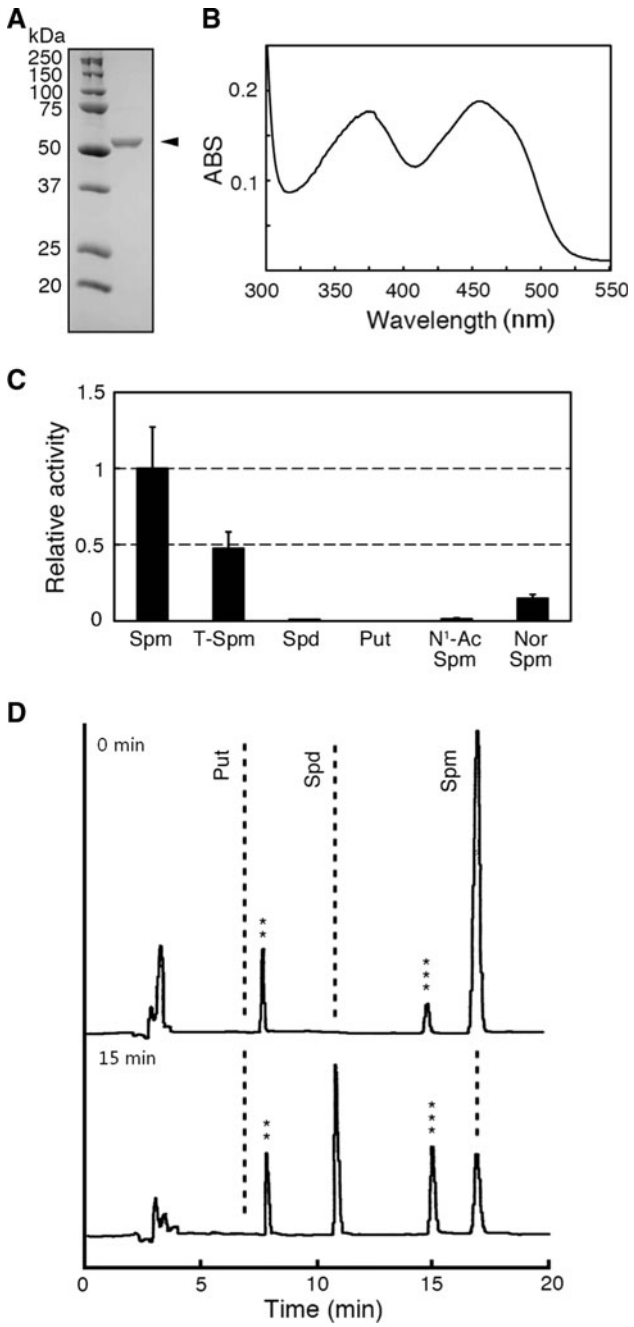

Fig. 4 Biochemical characteristics of OsPAO4. **a** Purification of the recombinant OsPAO4 protein on SDS–PAGE and visualized by CBB-staining. **b** Absorption spectrum of the purified OsPAO4 in a range of 300–540 nm. **c** PA specificity of the recombinant OsPAO4. The OsPAO4 enzyme activity was assessed by H_2O_2 production using the individual PAs as substrates. Activities were displayed relative to the one detected with Spm that was set as 1. **d** HPLC analysis of the reaction products catalyzed by OsPAO4 when Spm was used as a substrate

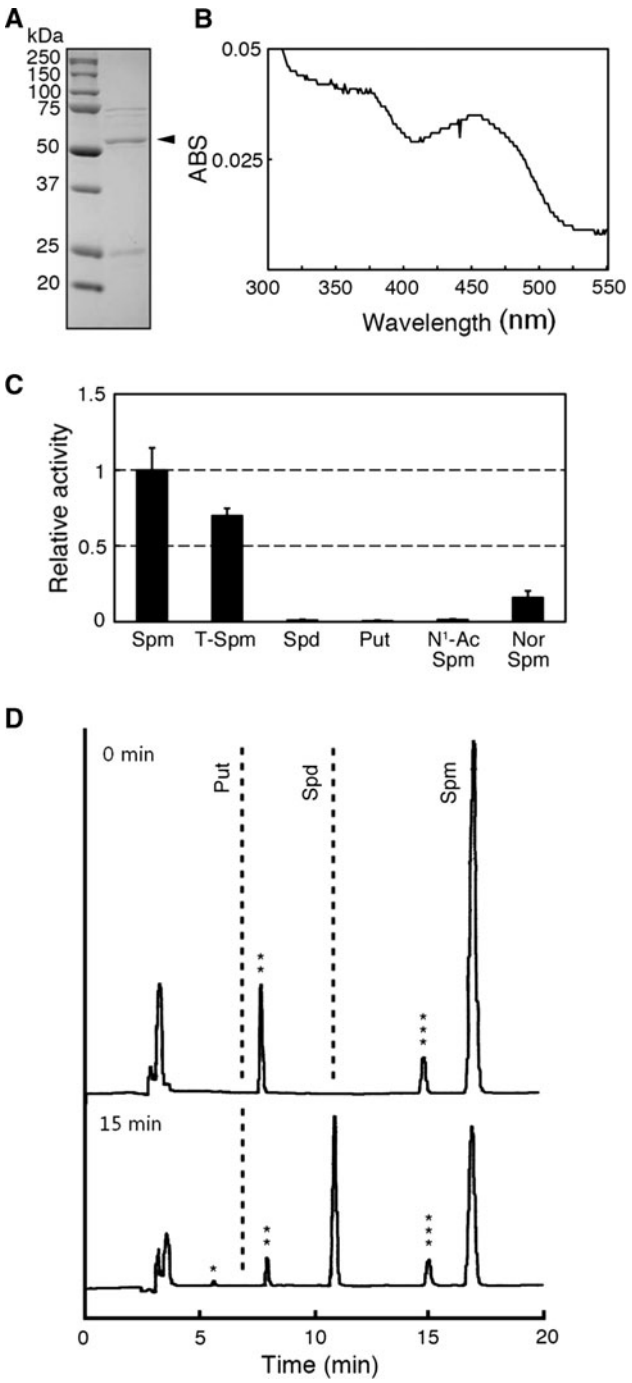

Fig. 5 Biochemical features of OsPAO5. **a** Purification of the recombinant OsPAO5 protein on SDS–PAGE and visualized by CBB-staining. **b** Absorption spectrum of the purified OsPAO5 in a range of 300–540 nm. **c** PA specificity of the recombinant OsPAO5. The OsPAO5 enzyme activity was assessed by H_2O_2 production using the individual PAs as substrates. Activities were displayed relative to the one detected with Spm that was set as 1. **d** HPLC analysis of the reaction products catalyzed by OsPAO5 when Spm was used as a substrate

HvPAO2 localizes in vacuoles (Cervelli et al. 2004, 2006; Cona et al. 2005). Involvement of ZmPAO in wound healing was indicated (Angelini et al. 2008). In contrast to the clade II *OsPAO* members, *OsPAO3*, *OsPAO4*, and *OsPAO5,* which belong to clade IV, were constitutively expressed at high levels (Fig. 2).

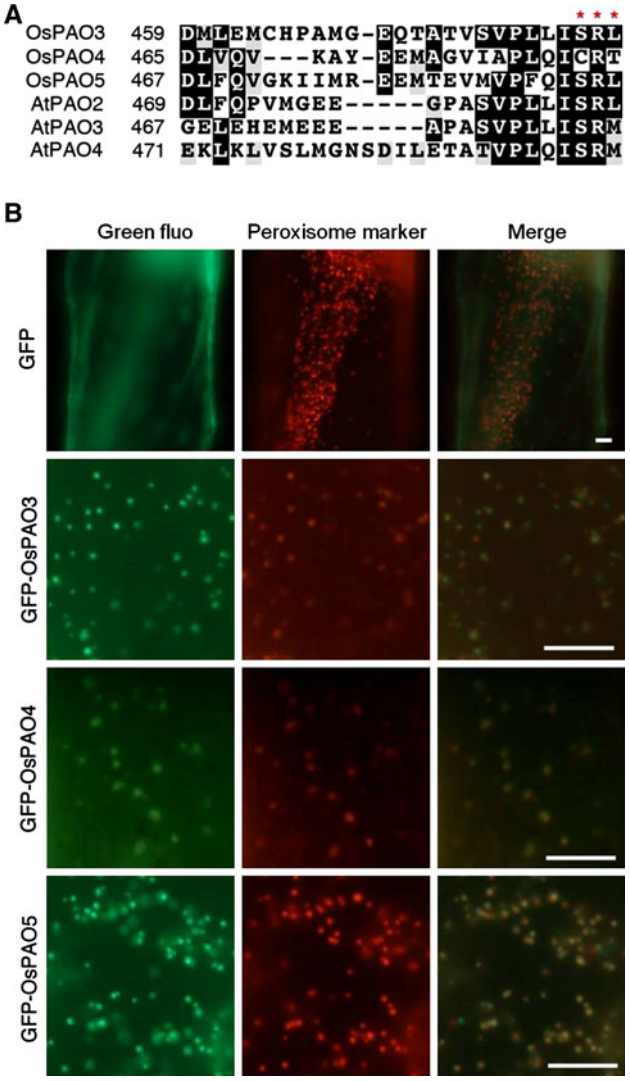

Fig. 6 Subcellular localization of OsPAO3, OsPAO4, and OsPAO5 in onion epidermal cells. **a** Putative peroxisome-targeting signal tripeptide sequences located in the C-termini of six members of rice and Arabidopsis PAOs (OsPAO3 to OsPAO5 and AtPAO2 to AtPAO4) are highlighted by red asterisks. **b** Peroxisomal localization of GFP-OsPAO3, GFP-OsPAO4, and GFP-OsPAO5 in onion epidermal cells. pGFP2 was used as GFP control. Green fluorescence derived from GFP-OsPAO3, GFP-OsPAO4, and GFP-OsPAO5 was co-localized with red fluorescence derived from mCherry-AtPAO3, a positive marker of peroxisome. *Bar* = 10 μm

Escherichia coli expressed OsPAO3 protein preferred Spd > T-Spm > Spm and had a full PA back-conversion activity (Fig. 3). OsPAO4 and OsPAO5 showed similar preference for PA substrates, i.e., Spm and T-Spm but not Spd, and Put was a good substrate. All the recombinant proteins—OsPAO3, OsPAO4, and OsPAO5—were able to carry out PA back conversion. Further, peroxisomal localization of OsPAO3, OsPAO4, and OsPAO5 was demonstrated (Fig. 6). It is likely that plant PAOs localized in peroxisomes function in PA back conversion.

OsPAO4 has a C-terminal tripeptide, CRT, which has not been verified as a functional plant PTS1 (Babujee et al. 2010; Reumann et al. 2007). Our results indicate that the C-terminus tricopeptide of CRT may be a functional motif of PTS1.

We propose a relationship between PAO clade and PA catabolism reaction mode. Clade I contains PAO members from dicotyledonous plants, while clade II those from monocotyledonous plants; clades III and IV are common to mono- and dicotyledonous PAO members. Previously, AtPAO2, AtPAO3, and AtPAO4 of the clade IV were shown to catalyze PA back-conversion reactions (Fincato et al. 2011; Kamada-Nobusada et al. 2008; Moschou et al. 2008; Takahashi et al. 2010). Here, we presented evidence that three rice PAOs, OsPAO3 to OsPAO5, belonging to clade IV, may function in PA back conversion (Figs. 3, 4, 5). Fincato et al. (2011) detected the PA back-conversion activity in *N. tabacum* cells. To consolidate a link between members of clade I and PA back-conversion activity, it will be necessary to characterize the reaction processes catalyzed by NtPAO and other clade I members such as MdPAO. Maize and barley PAOs (ZmPAO and HvPAO, respectively) that belong to clade II and shown to oxidize PA in the reaction of terminal catabolism (Cona et al. 2006). We hypothesize that OsPAO2, OsPAO6, and OsPAO7, which are classified into clade II, may be involved in terminal catabolism of PAs.

Acknowledgments We thank to Drs. K. A. Roubelakis-Angelakis and N. -H. Chua for kindly providing mCherry-AtPAO3 and pGFP2 plasmids, respectively. We also thank to Dr. E. Agostinelli and the anonymous reviewer(s) who contributed to improving this manuscript. This work was supported in part by Grant-in-Aids from the Japan Society for the Promotion of Science (JSPS) to TK (21380063) and YT (21780087, 23780345), and by the research funding program "LOEWE—Landes-Offensive zur Entwicklung Wissenschaftlich-ökonomischer Exzellenz" of Hesse's Ministry of Higher Education, Research, and the Arts to TB.

References

Alcázar R, Altabella T, Marco F, Bortolotti C, Reymond M, Koncz C, Carrasco P, Tiburcio AF (2010) Polyamines: molecules with regulatory functions in plant abiotic stress tolerance. Planta 231:1237–1249

Angelini R, Tisi A, Rea G, Chen MM, Botta M, Federico R, Cona A (2008) Involvement of polyamine oxidase in wound healing. Plant Physiol 146:162–177

Babujee L, Wurtz V, Ma C, Lueder F, Soni P, van Dorsselaer A, Reumann S (2010) The proteome map of spinach leaf peroxisomes indicates partial compartmentalization of phylloquinone (vitamin K1) biosynthesis in plant peroxisomes. J Exp Bot 61:1441–1453

Bagni N, Tassoni A (2001) Biosynthesis, oxidation and conjugation of aliphatic polyamines in higher plants. Amino Acids 20:301–317

Bassard J-E, Ullman P, Bernier F, Werck-Reichhart D (2010) Phenolamides: bridging polyamines to the phenolic metabolism. Phytochemistry 71:1808–1824

Binda C, Coda A, Angelini R, Federico R, Ascenzi P, Mattevi A (1999) A 30-Å-long U-shaped catalytic tunnel in the crystal structure of polyamine oxidase. Structure 7:265–276

Cervelli M, Tavladoraki P, Di Agostino S, Angelini R, Federico R, Mariottini P (2000) Isolation and characterization of three polyamine oxidase genes from *Zea mays*. Plant Physiol Biochem 38:667–677

Cervelli M, Cona A, Angelini R, Polticelli F, Federico R, Mariottini P (2001) A barley polyamine oxidase isoform with distinct structural features and subcellular localization. Eur J Biochem 268:3816–3830

Cervelli M, Di Caro O, Di Penta A, Angelini R, Federico R, Vitale A, Mariottini P (2004) A novel C-terminal sequence from barley polyamine oxidase is a vacuolar sorting signal. Plant J 40:410–418

Cervelli M, Bianchi M, Cona A, Crosatti C, Stanca M, Angelini R, Federico R, Mariottini P (2006) Barley polyaine oxidase isoforms 1 and 2, a peculiar case of gene duplication. FEBS J 38:667–677

Cohen SS (1998) A guide to the polyamines. Oxford University Press, Oxford

Cona A, Moreno S, Cenci F, Federico R, Angelini R (2005) Cellular redistribution of flavin-containing polyamine oxidase in differentiating root and mesocotyl of *Zea mays* L. seedlings. Planta 221:265–276

Cona A, Rea G, Angelini R, Federico R, Tavladoraki P (2006) Functions of amine oxidases in plant development and defence. Trends Plant Sci 11:80–88

Federico R, Angelini R (1991) Polyamine catabolism in plants. In: Slocum RD, Flores HE (eds) Biochemistry and physiology of polyamines in plants. CRC Press, Boca Raton, pp 41–56

Fincato P, Moschou PN, Spedaletti V, Tavazza R, Angelini R, Federico R, Roubelakis-Angelakis KA, Tavladoraki P (2011) Functional diversity inside the Arabidopsis polyamine oxidase gene family. J Exp Bot 62:1155–1168

Fuell C, Elliot KA, Hanfrey CC, Franceschetti M, Michael AJ (2010) Polyamine biosynthetic diversity in plants and algae. Plant Physiol Biochem 48:513–520

Groppa MD, Benavides MP (2008) Polyamines and abiotic stress: recent advances. Amino Acids 34:35–45

Hanzawa Y, Takahashi T, Michael AJ, Burtin D, Long D, Pineiro M, Coupland G, Komeda Y (2000) *ACAULIS5*, an *Arabidopsis* gene required for stem elongation, encodes a spermine synthase. EMBO J 19:4248–4256

Hanzawa Y, Imai A, Michael AJ, Komeda Y, Takahashi T (2002) Characterization of the spermidine synthase-related gene family in *Arabidopsis thaliana*. FEBS Lett 527:176–180

Kakehi J, Kuwashiro Y, Niitsu M, Takahashi T (2008) Thermospermine is required for stem elongation in *Arabidopsis thaliana*. Plant Cell Physiol 49:1342–1349

Kamada-Nobusada T, Hayashi M, Fukazawa M, Sakakibara H, Nishimura M (2008) A putative peroxisomal polyamine oxidase, AtPAO4, is involved in polyamine catabolism in *Arabidopsis thaliana*. Plant Cell Physiol 49:1272–1282

Knott JM, Romer P, Sumper M (2007) Putative spermine synthases from *Thalassiosira pseudonana* and *Arabidopsis thaliana* synthesize thermospermine rather than spermine. FEBS Lett 581:3081–3086

Kumar S, Dudley J, Nei M, Tamura K (2008) MEGA: a biologist-centric software for evolutionary analysis of DNA and protein sequences. Briefings in Bioinformatics 9:299–306

Kusano T, Berberich T, Tateda C, Takahashi Y (2008) Polyamines: essential factors for growth and survival. Planta 228:367–381

Lim TS, Chitra TR, Han P, Pua EC, Yu H (2006) Cloning and characterization of *Arabidopsis* and *Brassica juncea* flavin-containing amine oxidases. J Exp Bot 57:4155–4169

Mattoo AK, Minocha SC, Minocha R, Handa AK (2010) Polyamines and cellular metabolism in plants: transgenic approaches reveal different responses to diamine putresciner versus higher polyamines spermidine and spermine. Amino Acids 38:405–413

Moschou PN, Sanmartin M, Andriopoulou AH, Rojo E, Sanchez-Serrano JJ, Roubelakis-Angelakis KA (2008) Bridging the gap between plant and mammalian polyamine catabolism: a novel peroxisomal polyamine oxidase responsible for a full back-conversion pathway in Arabidopsis. Plant Physiol 147:1845–1857

Naka Y, Watanabe K, Sagor GHM, Niitsu M, Pillai A, Kusano T, Takahashi Y (2010) Quantitative analysis of plant polyamines including thermospermine during growth and salinity stress. Plant Physiol Biochem 48:527–533

Reumann S, Babujee L, Ma C, Wienkoop S, Siemsen T, Antonicelli GE, Rasche N, Lüder F, Weckwerth W, Jahn O (2007) Proteome analysis of Arabidopsis leaf peroxisomes revels novel targeting peptides, metabolic pathways, and defense mechanisms. Plant Cell 19:3170–3193

Seiler N (2004) Catabolism of polyamines. Amino Acids 26:217–233

Tabor CW, Tabor H (1985) Polyamines in microorganisms. Microbiol Rev 49:81–99

Takahashi Y, Cong R, Sagor GHM, Niitsu M, Berberich T, Kusano T (2010) Characterization of five polyamine oxidase isoforms in *Arabidopsis thaliana*. Plant Cell Rep 29:955–965

Tassoni A, Van Buuren M, Franceschetti M, Fornale IS, Bagni N (2000) Polyamine content and metabolism in *Arabidopsis thaliana* and effect of spermidine on plant development. Plant Physiol Biochem 38:383–393

Tavladoraki P, Shinina ME, Cecconi F, Di Agostino S, Manera F, Rea G, Mariottini P, Federico R, Angelini R (1998) Maize polyamine oxidase: primary structure from protein and cDNA sequencing. FEBS Lett 426:62–66

Tavladoraki P, Rossi MN, Saccuti G, Perez-Amador MA, Polticelli F, Angelini R, Federico R (2006) Heterologous expression and biochemical characterization of a polyamine oxidase from Arabidopsis involved in polyamine back conversion. Plant Physiol 141:1519–1532

Thompson JD, Higgins DG, Gibson TJ (1994) CLUSTAL W: improving the sensitivity of progressive multiple sequence alignment through sequence weighting, position-specific gap penalties and weight matrix choice. Nucleic Acid Res 22:4673–4680

Vujcic S, Diegelman P, Bacchi CJ, Kramer DL, Porter CW (2002) Identification and characterization of a novel flavin-containing spermine oxidase of mammalian cell origin. Biochem J 367:665–675

Vujcic S, Liang P, Diegelman P, Kramer DL, Porter CW (2003) Genomic identification and biochemical characterization of the mammalian polyamine oxidase involved in polyamine back-conversion. Biochem J 370:19–28

Wallace HM, Fraser AV, Hughes A (2003) A perspective of polyamine metabolism. Biochem J 376:1–14

Wang Y, Devereux W, Woster PM, Stewart TM, Hacker A, Casero RA Jr (2001) Cloning and characterization of a human polyamine oxidase that is inducible by polyamine analogue exposure. Cancer Res 61:5370–5373

Wu T, Yankovskaya V, McIntire WS (2003) Cloning, sequencing, and heterologous expression of the murine peroxisomal flavoprotein, N^1-acetylated polyamine oxidase. J Biol Chem 278:20514–20525

Yoda H, Hiroi Y, Sano H (2006) Polyamine oxidase is one of the key elements for oxidative burst to induce programmed cell death in tobacco cultured cells. Plant Physiol 142:193–206

Zolman BK, Bartel B (2004) An Arabidopsis indole-3-butyric acid-response mutant defective in PEROXIN6, an apparent ATPase implicated in peroxisomal function. Proc Natl Acad Sci U S A 101:1786–1791